ACCELERATION AND TRANSPORT OF ENERGETIC PARTICLES AT CME-DRIVEN SHOCKS

G. Li [1], G.P. Zank[1], and W.K.M. Rice [2]

[1] *IGPP, University of California, Riverside, CA 92521 USA*
[2] *University of St. Andrews, St. Andrews, Fife KY16 9SS, Scotland*

ABSTRACT

Historically, solar energetic particle (SEP) events are classified in two classes as "impulsive" and "gradual". Whether there is a clear distinction between the two classes is still a matter of debate, but it is now commonly accepted that in large "gradual" SEP events, Fermi acceleration, also known as diffusive shock acceleration, is the underlying acceleration mechanism. At shock waves driven by coronal mass ejections (CMEs), particles are accelerated diffusively at the shock and often reach > MeV energies (and perhaps up to GeV energies). As a CME-driven shock propagates, expands and weakens, the accelerated particles can escape ahead of the shock into the interplanetary medium. These escaping energized particles then propagate along the interplanetary magnetic field, experiencing only weak scattering from fluctuations in the interplanetary magnetic field (IMF). In this paper, we use a Monte-Carlo approach to study the transport of energetic particles escaping from a CME-driven shock. We present particle spectra observed at 1 AU. We also discuss the particle "crossing number" at 1AU and its implication to particle anisotropy. Based on previous models of particle acceleration at CME-driven shocks, our simulation allows us to investigate various characteristics of energetic particles arriving at various distances from the sun. This provides us an excellent basis for understanding the observations of high-energy particles made at 1 AU by ACE and WIND.

INTRODUCTION

Measurements of the abundance of ion charge states (see for example, *Mason et al.*, 1995; *Tylka et al.* 1995; *Oetliker et al.*, 1997) indicate that the gradual SEP events are associated with a temperature of T $\approx 2 \times 10^6$ K. This is consistent with ions being accelerated from coronal material. It thus naturally leads to the idea that gradual Solar Energetic Particles (SEPs) events result from particle acceleration at CME-driven coronal and interplanetary shocks (see reviews by *Reames* 1995,1999, *Cane* 1995, *Gosling* 1993 and *Cliver and Cane* 2002).

The commonly accepted mechanism of particle acceleration at a shock is first-order Fermi, also known as diffusive shock acceleration (see for example, *Axford et al.*, 1977). Here particles scatter back and forth between the upstream and downstream medium due to magnetic turbulence such as Alfv́en waves. Upon completing each traversal, a (non-relativistic) particle will gain a momentum proportional to $m\Delta v$, where m is the particle mass and $\Delta v = |v_2 - v_1|$ is the background velocity difference between the upstream and downstream. For a propagating CME-driven shock, Alfv́en waves are driven by protons streaming off the shock front and the wave intensity is coupled to the anisotropic part of the particle distribution function f. Thus, a self-consistent model on particle acceleration and transport requires evaluating the wave intensity simultaneously with f. In this work, we follow the approach of *Gordon et al.* (1999) to evaluate the wave intensity at the shock front. We then assume that at some distances in front of the shock, the turbulence

becomes negligible and the escaped particles will only experience occasional pitch angle scattering due to fluctuations of IMF and the transport thus obeys the Boltzmann equation. Works which consider the effects of proton excited waves on the transport of various ions can be found, for example in *Ng et al.* (1999).

In an earlier work, *Zank et al.* (2000) modeled a CME-driven shock numerically and studied particle acceleration at the shock. They showed that particles can be accelerated up to $\sim$ GeV energies by a strong shock at the early stage of the shock propagation while close to the Sun. The accelerated particles can escape upstream from the shock. Upon leaving the shock, particles gyrate along the interplanetary magnetic field, described by a Parker spiral; with occasional pitch angle scatterings. The transport of these particles is the main focus of this paper. We use a Monte-Carlo approach to follow individual particle trajectories. All macroscopic quantities, such as the particle intensity, spectrum and momentum distribution observed at 1 AU are obtained by summing over all individual events. The Monte-Carlo approach allows us to investigate the particle average crossing number, *Rc*.

We note that understanding the characteristics of these high energy particles is also of great practical interests. Indeed, the detection of SEP's could provide us a way of predicting shock characteristics, such as propagation speed, direction and strength. Furthermore, high energy particles entering the polar atmosphere can modify atmospheric chemistry, leading to possible ozone zone depletion (*Jackman et al. 2001*).

MODEL DESCRIPTION

Acceleration

Zank et al. (2000) used a one-dimensional hydrodynamic code to model the evolution of a CME-driven shock wave. In this approach, the region that the CME sweeps is approximated by a series of concentric shells. The shock fronts corresponds to the outermost shell. All the shock properties, such as shock speed and compression ratio, are calculated numerically as the shock wave expands. At the shock front, the accelerated particle spectrum is produced by diffusive shock acceleration with a simplified form of the diffusion coefficient, the Bohm limit. The use of the Bohm limit is justified for strong shocks where magnetic turbulence is substantial. However, For shock waves of weaker strength, the Bohm limit predicts an unrealistically small diffusion coefficient. *Rice et al.* (2002) explicitly evaluate the diffusion coefficient under the assumption that the turbulence is primarily Alfv̀en waves generated by streaming protons. In this approach, the resonant wave number, given by the Doppler condition, then determines the appropriate diffusion coefficient. Detailed calculations verify that for strong shocks, the Bohm limit is recovered.

The maximum momentum (energy) achieved by the acceleration can be evaluated by equating the dynamical timescale and the acceleration time scale (*Drury*, 1983),

$$\frac{r(t)}{\dot{r}(t)} = \frac{q(t)}{V'^2}\int_{p_{inj}}^{p_{max}} \kappa_{rr}(p')d(ln(p')). \tag{1}$$

In eq. (1), $r(t)$ and $\dot{r}(t)$ are the shock location and the shock speed at time t in the laboratory/spacecraft frame. V' is the upstream flow speed in the stationary shock frame. p_{inj} and p_{max} are the particle injection and maximum momentum. $q(t)$ is the spectrum index of the accelerated particle and $\kappa_r(p)$, the diffusion coefficient, is evaluated by assuming that the turbulence responsible for particle scattering near the shock front is Alfv́en wave generated by streaming protons (see Gordon et al. 1999 and Rice et al., 2002). As a simple estimate, we follow *Völk et al.* (1988) and *Zank et al.* (2000) by assuming that p_{inj} is some fraction of the downstream thermal energy per particle, thus

$$p_{inj} = \left[\frac{3\alpha(\gamma-1)\rho_1(t)\dot{r}^3(t)}{2\gamma n_2(t)u_2(t)}\right]^{1/2}\left\{1-\left(\frac{\rho_1(t)}{\rho_2(t)}\right)^2+\frac{2}{(\gamma-1)M_1^2(t)}\right\}^{1/2} \tag{2}$$

Here, α is a parameter taken to be 0.5 in this simulation. $\gamma = 5/3$ is the gas adiabatic. $\rho_1(t)$ ($\rho_2(t)$) is the upstream (downstream) mass density. $M_1(t)$ is the upstream Mach number. $n_2(t)$ and $u_2(t)$ are the downstream number density and fluid speed. From p_{inj} and p_{max}, the local accelerated particle spectrum at the shock front is then,

$$f(p) \sim p^{\frac{3s(t)}{s(t)-1}} \qquad (p_{inj} < p < p_{max}) \tag{3}$$

Behind the shock front, accelerated particles cool, convect, and diffuse. This is modeled as the basis of the shell model (*Zank et al.*, 2000) and the spectrum is changing with time, as particles can move between different shells.

Transport

Energetic particles escaping from the shock front into the interplanetary medium obey the Boltzmann-Vlasov equation,

$$\frac{\partial f}{\partial t} + \frac{\mathbf{p}}{m} \cdot \nabla f + \mathbf{F} \cdot \nabla_p f = \left. \frac{\partial f}{\partial t} \right|_{coll}. \tag{4}$$

Here $f(r, p, t)$ is the particle phase space distribution function. The right hand side of (4) describes particle collisions. For charged particles propagating in solar wind, the collisions are mainly due to the scattering on fluctuations of the interplanetary magnetic field (IMF). Within the frame work of quasi-linear theory, this term is given by $\frac{\partial}{\partial \mu}(D_{\mu\mu}\frac{\partial f}{\partial \mu})$, where $D_{\mu\mu}$ is the corresponding Fokker-Plank coefficient.

Between two consecutive pitch angle scatterings, charged particles move in the solar wind by gyrating along a field line. As the magnetic field expands radially, particles will experience adiabatic cooling and focusing effects as a consequence of adiabatic invariants of the motion. The geometry of the magnetic field $\mathbf{B}$ is given by the usual Parker spiral (*Parker* 1958),

$$B = B_0(\frac{R_0}{r})^2[1 + (\frac{\Omega_0 R_0}{u})(\frac{r}{R_0} - 1)^2 sin^2\theta]^{1/2}, \tag{5}$$

where θ is the colatitude of the solar wind with respect to the solar rotation axis. Ω_0 is the solar rotation rate, u is the radial solar wind speed, and B_0 is the interplanetary magnetic field (IMF) at the co-rotation radius R_0 (typically, $R_0 = 10R_\odot$, $B_0 = 1.83 \times 10^{-6}T$, $u = 400km/s$, and $\Omega_0 = 2\pi/25.4$days). The components of $\mathbf{B}$ along $\hat{\mathbf{r}}$ and $\hat{\phi}$, B_r and B_ϕ respectively, satisfy

$$\frac{dr}{B_r} = \frac{r\sin\theta d\phi}{B_\phi}. \tag{6}$$

Considering the equatorial plane, where $\theta = \pi/2$, we then get the path length ds of the particle along the B field line,

$$ds = \sqrt{dr^2 + (rd\phi)^2} = \sqrt{1 + (B_\phi/B_r)^2}dr. \tag{7}$$

Equation (7) describes the "free" motion of a charged particle between pitch angle scatterings. The duration of this "free" motion is given by the mean free path $\lambda_{//}$. Following *Zank et al.* (1998) and *Li et al.* (2003), we may express the particle mean free path as,

$$\lambda = \lambda_0(\frac{pc}{1\mathrm{GeV}})^\alpha(\frac{r}{1\mathrm{AU}})^\beta \tag{8}$$

where λ_0, is an input parameter and taken to be 0.4 AU here. The parameters α and β describe the momentum and heliocentric distance dependence, and are taken to be 1/3 for α and 2/3 for β.

In our simulation, we follow the motion of individual charged particles when they escape from shock front. Thus, we need to know the position of the shock as a function of time and the phase space distribution of the energetic particles at the shock front. Following the approach as described in the section **Acceleration**, the accelerated particle distribution function $f(r(p,t),p,t)$ is obtained for a series of times t_1, t_2, ... , t_n. Integrating $f(r(t),p,t)$ over p^2dp, we have

$$N(t) = \int f(r(t),p,t)p^2dp, \tag{9}$$

and $N(t)$ is the function from which we sample the escape time of our initial particles (and thus location). For a given random number ξ $(0 \leq \xi \leq 1)$, the following equation

$$\frac{\int_{t_s}^{t} N(t')dt'}{\int_{t_s}^{t_e} N(t')dt'} = \xi \tag{10}$$

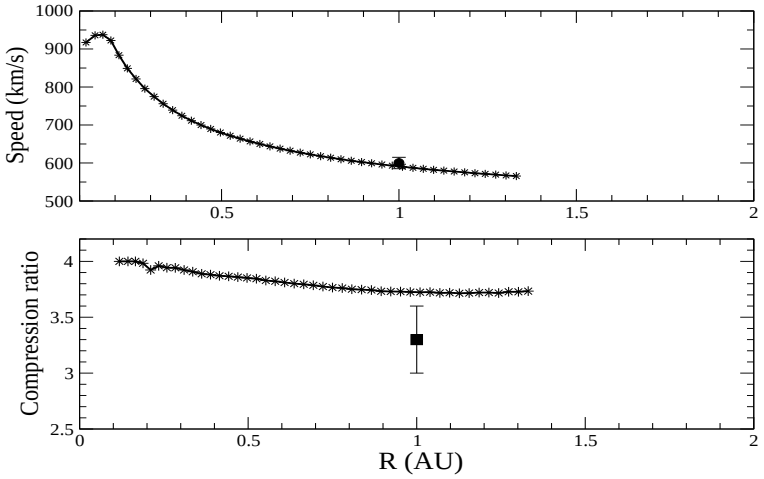

Fig. 1. The shock properties. The upper panel shows the shock velocity as a function of heliodistance. The lower panel shows the compression ratio s. The shock is initially strong with $s = 4$ and a speed ~ 950 km/s, and weakens to $s = 3.7$ and $v \sim 620$ at 1 AU. Typical values of solar wind speed and compression ratio observed at 1 AU are also indicated in the figure with error bars. See text for details.

determines t, which is the time for a test particle leaving the shock. In the above, t_s and t_e denote the time at which the shock starts and the time when the shock reaches 1 AU. Once t is determined, the momentum of the particle can be determined in a similar way through,

$$\frac{\int_{p_{inj}}^{p} f(r(q,t),q,t)q^2dq}{\int_{p_{inj}}^{p_{max}} f(r(q,t),q,t)q^2dq} = \xi', \tag{11}$$

where ξ' $(0 \leq \xi \leq 1)$ is another independent random variable. It is clear that From (10) and (11), it is clear that the sampling of particle escaping time t is weighted according to $N(t)$, and the sampling of p is weighted accoring to $f(p)p^2$.

After the initial condition (t,p) of a test particle is decided, its subsequent motion is simply an interplay between "free" motion and pitch angle scatterings. The scatterings themselves are assumed to be isotropic and Markovian, thus the new pitch angle after a scattering has no memory of the previous pitch angle.

RESULTS

We consider a simulation of a weak shock. The CME driven shock is introduced at 0.1 AU, where the solar wind is supersonic, by temporarily increasing the number density and solar wind velocity by a factor of 3.25 for half an hour. This corresponds to an energy injection of the order 10^{32} erg, a typical value for a coronal mass ejection. We assume $\gamma = 5/3$ to model the solar wind. The weak shock has an initial velocity of 950km/s and drops to about 620km/s at 1 AU, taking ~ 51 hours to reach 1 AU.

Fig. 1 plots the shock properties. The upper panel plots the shock velocity as a function of heliodistance. The lower panel is the compression ratio s. Typical values of the shock velocity and the compression ratio at 1 AU from observations are also shown in the figure as the two dots with an error bar (*Desai et al.* 2002).

Fig. 2 shows particle spectra at 1 AU for different time intervals. Particles arriving at 1 AU are binned into 250 energy bins. A total of $5 * 10^7$ particles are followed in this calculation. As opposed to the unit $(cm^2 ssr MeV)^{-1}$, used in observations, Figure 2 plots the relative intensity instead. The time evolution of the spectrum is clearly seen. At earlier times, more high energy particles are observed at 1 AU due to their greater velocities, seen from the curves in the lower right corner of the figure. At later times, more low energy particles cross 1 AU and the number of high energy particles begin to decrease as the shock weakens. The curves then evolve to those shown in the upper left corner. The solid curves, from the lower right corner to the upper left corner, correspond to $0 - 2.52$ hours, $10.08 - 12.60$ hours, $22.68 - 25.20$ hours,

35.28 – 37.80 hours and 47.88 – 50.40 hours. The uppermost solid curve is the time integrated spectrum from shock initiation until it reaches 1 AU. It is an approximate power law with a break (bump) around 10 MeV. The spectrum index is roughly ~ 1.6. Note a $f(p) \sim p^{\alpha}$ corresponds to $f(T) \sim T^{\beta}$ with $\beta = \frac{\alpha+1}{2}$. Using $\alpha = 3s/(s-1)$, we find $\beta = 1.5$ for $s = 4$ and $\beta = 1.555$ for $s = 3.7$. This is in good agreement with our simulation. Such spectral index is also seen observationally (*Tylka* 2002). The spectra at different times are also approximate power laws with a "broken-feature". For example, at time 10.08 – 12.60 hours, the spectrum for particles above $T = 70$ MeV begins to deviate from the power law, suggesting that the shock is no longer accelerating particles to that energy. Similarly, at 35.28 – 37.80 hours, at energies above $T = 20$ MeV, a deviation from the power law becomes noticeable.

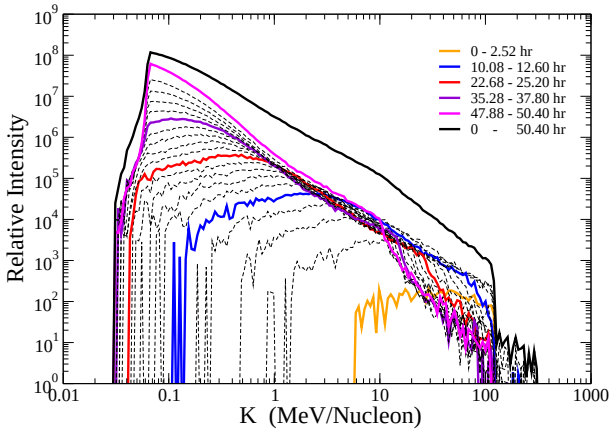

Fig. 2. The particle spectrum observed at 1 AU as a function of time. Each curve represent a distinctive time period. The uppermost curve is the time integrated spectrum. Other solid curves, from lower right corner to the upper left corner, correspond to 0 – 2.52 hours, 10.08 – 12.60 hours, 22.68 – 25.20 hours, 35.28 – 37.80 hours and 47.88 – 50.40 hours.

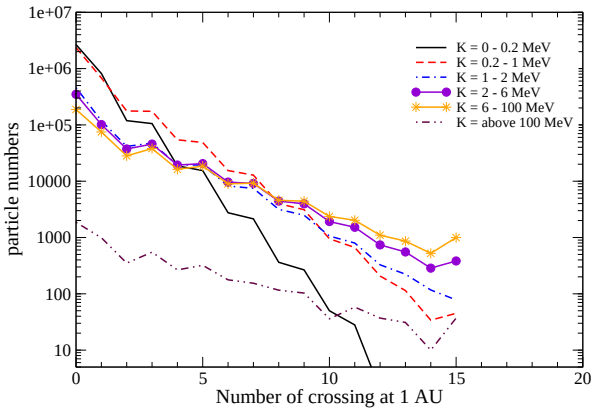

Fig. 3. The distribution of particles as a function of the number of crossings at 1 AU for different energies before the shock arrival. See text for details.

As shown in *Li et al.* (2003), particles can cross 1 AU multiple times. The number of crossings depends on particle energy. Higher energy particles cross 1 AU more often than lower energy particles. Fig. 3 plots the particle number as a function of crossing number. It is clear from the figure that particles have a broad distribution of crossing numbers. Multiple crossings are important for understanding the observations of energetic particles. For example, a particle having a crossing number of 2 indicates that it crosses 1 AU along $\hat{r}$ direction at an earlier time and crosses 1 AU along $-\hat{r}$ direction at a later time and then absorbed by the shock front. Similarly, a particle having a crossing number of 3 must cross 1 AU along $\hat{r}$ direction twice and cross 1 AU along $-\hat{r}$ direction once. At crossing number above five, there are more particles within the energy bin of 1 – 2 MeV than those of 0 – 0.2 MeV. This is due to the fact that lower energy particles have smaller speed and are easily caught by the expanding shock.

CONCLUSION

We have investigated the acceleration and transport of energetic particles at CME-driven shocks. The acceleration is modeled numerically using a shell model, with the shock modeled by a MHD code. The particle transport is studied using a Monte Carlo code, where single particle trajectories are followed. Particle spectra at 1 AU is then calculated. The time evolution of the spectra is shown in Figure 2. A power law feature is clearly seen. As time evolves and the shock expands and weakens, the power law spectra becomes "broken" at lower energies. The time integrated spectrum is also approximately a power law with

a spectral index in agreement with observations. We have also calculated the distribution of the particle crossing numbers at 1 AU. We find that particles can cross 1 AU multiple times and higher energy particles have a larger average crossing number than lower energies. The number of crossings has a broad distribution and some high energy particles can cross 1 AU more than 15 times before the shock reaches 1AU.

ACKNOWLEDGMENTS

This work has been supported in part by a NASA grant NAG5-10932 and an NSF grant ATM-0296113.

REFERENCES

Axford, W. I., E. Leer, and G. Skadron, Proc. 15th Int. *Cosmic Ray Conf. (Plovdiv)*, **11**, 132-137, 1978.

Cane, H. V., The structure and evolution of interplanetary shocks and the relevance for particle-acceleration, *Nucl. Phys. B.*,**39A**, 35-44, 1995.

Cliver, E. W., H. V. Cane, Gradual and Impulsive Solar Energetic Particle Events, *EOS*, **83**, number 7, 2002.

Desai, M., G. M. Mason, private communication, 2002.

Drury, L.O'C., An introduction to the theory of diffusive shock acceleration of energetic particles in tenuous plasmas, *Rep. Prog. Phys.*, **46**, 973-1027, 1983.

Gordon, B. E., M. A. Lee, and E. Möbius, Coupled hydromagnetic wave excitation and ion acceleration at interplanetary traveling shocks and Earth's bow shock revisited, *J. Geophys. Res.*, **104**, 28263-28277, 1999.

Gosling, J. T., The solar-flare myth, *J. Geophys. Res.*, **98**, 18937-18949, 1993.

Jackman, C. H.; R. D. McPeters; G. J. Labow; E. L. Fleming; C. J. Praderas; J. M. Russell, Northern Hemisphere atmospheric effects due to the July 2000 solar proton event interstellar pickup ions, *Geophys. Res. Lett.*, **28**, p.2883-2886, 2001.

Li, G., G. P. Zank and W. K. M. Rice, Energetic particle acceleration and Transport at coronal mass ejection drive shocks, *J. Geophys. Res.*, **108(A2)**, 1082, doi:10.1029/2002JA009666, 2003.

Mason, G. M., J. E. Mazur, M. D. Looper, and R. A. Mewaldt, Charge-state measurements of solar energetic particles observed with SAMPEX, *Astrophys. J.*, **452**, 901-911, 1995.

Ng, C. K., D. V. Reames, and A. J. Tylka, Effect of proton-amplified waves on the evolution of solar energetic particle composition in gradual events, *Geophys. Res. Lett.*, **26**, 2145-2148, 1999.

Oetliker, M., B. Klecker, D. Hovestadt, G. M. Mason, J. E. Mazur, R. A. Leske, R. A. Mewaldt, J. B. Blake, and M. D. Looper, The ionic charge of solar energetic particles with energies of 0.3-70 MeV per nucleon, *Astrophys. J.*, **477**, 495-501, 1997.

Parker, E. N., Dynamics of the interplanetary gas and magnetic fields, *Astrophys. J.*, **123**, 664-676, 1958.

Reames, D. V., Coronal abundances determined from energetic particles, *Adv. Space Res.*, **15**, 41-51, 1995.

Reames, D. V., Particle acceleration at the Sun and in the heliosphere, *Space Sci. Rev.*, **90**, 413-491, 1999.

Rice, W. K. M., G. P. Zank and G. Li, Particle acceleration at coronal mass ejection drive shocks: for arbitrary shock strength. Submitted to *J. Geophys. Res. (Space)*, 2003.

Tylka, A. J., P. R. Boberg, J. H. Adams, L. P. Beahm, W. F. Dietrich, and T. Kleis, The mean ionic charge state of solar energetic Fe ions above 200 MeV per nucleon, *Astrophys. J.*, **444**, L109-L113, 1995.

Tylka, A.J., private communication, 2002.

Völk, H. J., L. A. Zank and G. P. Zank, Cosmic-ray spectrum produced by supernova-remnants with an upper limit on wave dissipation, *Astron Astrophys.*, **198**, 274-282, 1988.

Zank, G. P., W. K. M. Rice, and C. C. Wu, Particle acceleration and coronal mass ejection drive shocks: A theoretical model, *J. Geophys. Res. (Space)*, **105**, 25079-25095, 2000.

Zank, G. P., Matthaeus, W. H., Bieber, J. W., H. Moraal, The radial and latitudinal dependence of the cosmic ray diffusion tensor in the heliosphere, *J. Geophys. Res. (Space)*, **103**, 2085-2097, 1998.

E-mail address of G. Li ganli@citrus.ucr.edu

Manuscript received 21 November, 2002; revised 26 March, 2003; accepted 26 March, 2003